Proceedings World Geothermal Congress 2020+1
Reykjavik, Iceland, April - October 2021

Flow Field Characteristics of Swirling Abrasive Jet Nozzle for Geothermal Radial Jet Drilling

Xin LIU, Zhongwei HUANG*, Jingbin LI, Xiao HU

Center for Geothermal Energy, China University of Petroleum (Beijing), Beijing, 102249, China

Corresponding author. Email address: huangzw@cup.edu.cn (Z. Huang)

Keywords: RJD well; swirling jet; abrasive waterjet; twisted tape; geothermal reservoir

ABSTRACT

Radial jet drilling (RJD) technology is a viable alternative to drill multiple horizontal laterals outward from the main vertical wellbore, which is more efficient to exceed conventional hydraulic stimulation technology in geothermal resource exploitation. Swirling abrasive waterjet (SAWJ), generates by twisted tapes inside the nozzle, is one key technique of RJD to form the laterals efficiently. In this paper, the SAWJ flow field is investigated by numerical simulation, with twisted tapes of angle from 0°to 720°. The realizable k-epsilon model and Euler multiphase model were used. Introduced the swirl number S to denote the swirling intensity inside the nozzle. The velocity and dynamic pressure distribution water phase are discussed. Numerical simulation suggests that there is no potential core (velocity is constant in the center) that appeared in the stronger swirling jet area. On the sections normal to the jet axis, tangential and axial velocity component profiles are of M-shaped distribution, where impact energy concentrates into an annular shape. With the larger angle of the twisted tapes, the swirling flow generates by twisted tape is of greater tangential velocity and swirling intensity. After, the swirl decays along the jet axis. Swirling makes the distribution area of abrasive increase; each abrasive particle can be accelerated to three-dimensional velocity. On the impact surface, the dynamic pressure is larger with stronger swirling, makes it possible to drill holes in the geothermal reservoir efficiently. The investigation on SAWJ is of great significance for exploiting aquifer and hot dry rock (HDR) geothermal reservoirs.

1. INTRODUCTION

Recently, Radial Jet Drilling (RJD) technology has become an attractive well stimulation method technology for enhancing well productivity/injectivity in low-performing geothermal wells (Song et al. 2018). In the high fracture density formation, the RJD laterals can be effective in heat production by providing access to the hot rock. In low permeability reservoirs that the flow mainly occurs through the fracture network, the RJD laterals connect to the fracture network (Salimzadeh et al. 2019).12 laterals were jetted in geothermal injection wells in Lithuania, which resulted in an increase in production of 14% (Rohith NAIR et al. 2017). The RJD system pumps fluid under high pressure through the high-pressure hose and then exits the nozzle at a very high velocity. A larger diameter hole is drilled by the nozzle before the nozzle and tool assembly trip into the laterals. The diameter of these radials is approximately 1 to 2 inches (2.54 to 5.1 cm) (Ahmed 2017). The nozzle used in RJD is a key part since it breaks rock to form a horizontal hole. Engineering practice shows that the hole-enlarging capability and rock-breaking efficiency of the nozzle has become the main problems to be solved (Liao et al. 2020).

Fig. 1 Diagrammatic sketch of swirling jet

Abrasive water jet (AWJ) cutting is one of the non-traditional cutting processes capable of cutting a wide range of hard-to-soft materials. An abrasive jet uses a mixture of water and abrasive to more effectively cut through materials. AWJ process includes parameters of hydraulic pressure, traverse speed, stand-off distance, abrasive mass flow rate, abrasive materials, nozzle length and diameter, orifice diameter, abrasive shape, size, and hardness. Impact velocity is the most important variable in impact erosion, also impact angle is the second most important factor affecting material removal. Maximum erosion occurs at an impact angle near 90 degrees for brittle materials but the peak erosion angle is 20 to 30 degrees for ductile materials (Patel K and Shaikh A. 2015)(Al-Marahleh G 2015).

Swirling impinging jets have three unique regions, namely free jet, impingement, and wall jet regions. Swirling jets also display complex and distinguishable other flow features, such as flow reversal, often termed as vortex breakdown (Debnath et al. 2020) (Gupta et al. 1984). Fig. 1 shows a 3D simulation diagram of a swirling impinging jet. A swirling jet can be generated by a twisted tape in the jet nozzle. Compared to conventional impinging jet, swirling jet spreads more rapidly and widely and entrains the surrounding fluid at a greater rate. (Xu et al. 2017). Bang et al. Studied velocity components and the spray cone angle of swirling flow at the atomizer nozzle exit. The theoretical parametric studies include the effect of the internal nozzle geometry, the mass flow rate, and the effect of the swirling strength (Bang et al. 2020). Li et al. and Liu et al. studied the jets flow field of a self-propelled multi-orifice drilling bit, which generates a swirling flow to break rocks. Due to the rotational structure and small diameter nozzles, self-propelled multi-orifice drilling bits do not allow abrasive particles to pass. (Li et al. 2015) (Liu et al. 2020)

Although AWJ is with strong hard material breaking ability, there is also a defect of small hole diameter (Yang Yongyin et al. 1999). Comparing to conventional impinging jet, swirling jet spreads more rapidly and widely and entrains the surrounding fluid at a greater rate. Swirl jet technology can be used to combine with AWJ for rock-breaking applications (Yang Yongyin et al. 2005). The mixture of abrasive and water flows through the nozzle twisted tape, forced to swirl through the twisted tape, then exit from the nozzle to form a conical spreading jet. Thus, the characteristics of the swirl abrasive water jet (SAWJ) flow field has an effect on the nozzle design optimization for rock-breaking. Greater hole diameter is of great significance to the RJD laterals completion and the geothermal resource exploration.

In this paper, the numerical simulation of SAWJ nozzles with different geometric parameters is carried out, and the axial, tangential, and radial velocity distributions of the swirling abrasive jet are analyzed. In order to obtain the SAWJ impinging distribution, the abrasive and water dynamic pressure is extracted by the numerical simulation results. In order to study the characteristics of jet swirling and its generation and decay, the velocity distribution in the numerical simulation flow field is extracted, a calculation program was written to calculate the swirl number accurately in the internal and external flow field section of the nozzle.

2. MATHEMATICAL

2.1 Swirl flow theory

The swirling jet is equipped with a twisted tape setting inside the nozzle to make the jet flow swirl so as to increase the spreading capacity. Based on the assumption of axisymmetric, stable, incompressible and turbulent free jet boundary layer flows under un-submerged conditions, and ignoring the volume force and viscous force, a simplified differential governing equation for the self-similar flow of rotating jet flows suitable for the strength of small swirling flows can be obtained.

The governing equations in this current study are the conservation of mass, momentum, and energy. The equations are expressed in terms of the axisymmetric cylindrical coordinate system with constant fluid properties as:

$$\frac{\partial}{\partial x}(ru)+\frac{\partial}{\partial r}(rv)=0 \tag{1}$$

$$u\frac{\partial u}{\partial x}+v\frac{\partial u}{\partial r}=-\frac{1}{\rho}\frac{\partial p}{\partial x}-\frac{\partial}{\partial r}\overline{u'v'}-\frac{\partial}{\partial x}\overline{u'^2}-\frac{\overline{u'v'}}{r} \tag{2}$$

$$-\frac{\omega^2}{r}=-\frac{1}{\rho}\frac{\partial p}{\partial r}-\frac{\partial}{\partial r}\overline{v'^2}-\frac{\overline{v'^2}}{r}+\frac{\overline{\omega'^2}}{r} \tag{3}$$

$$u\frac{\partial \omega}{\partial x}+v\frac{\partial \omega}{\partial r}+\frac{v\omega}{r}=-\frac{1}{\rho}\frac{\partial p}{\partial x}-\frac{\partial}{\partial r}\overline{u'v'}-\frac{\partial}{\partial x}\overline{u'^2}-\frac{\overline{u'v'}}{r} \tag{4}$$

Where ρ the density of the fluid, x the axial coordinate, r the radial coordinate, u the axial velocity, v the radial velocity, and ω the tangential velocity.

Integral expressions of first-order approximate axial momentum G_x flux conservation and angular momentum G_Φ flux conservation:

$$G_x=2\pi\rho\int_0^\infty r\left(u^2-\frac{\omega^2}{2}\right)dr=const \tag{5}$$

$$G_\Phi=2\pi\rho\int_0^\infty r^2u\omega dr=const \tag{6}$$

Thus, denote swirl number S as:

$$S=\frac{\int_0^R r^2u\omega dr}{R\int_0^R\left(u^2-\frac{\omega^2}{2}\right)dr} \tag{7}$$

Where *R* the radius of the flow.

2.2 Numerical model

The realizable k- ε model proposed by (Shih et al. 1995) differs from the standard k- ε model which can be used in a wide range of flows (S.-E. Kim et al. 1997), including rotating homogeneous shear flows and free flows including jets and mixing layers. For all these cases, the performance of the model has been found to be substantially better than that of the standard k-ε model. Especially noteworthy is the fact that the realizable k-ε model resolves the round-jet anomaly; that is, it predicts the spreading rate for

axisymmetric jets as well as that for planar jets. The rock breaking depends on the spreading rate of the jet flow field; thus, this model is selected to study SAWJ.

3. NUMERICAL PROCEDURE

3.1 Geometry of twisted tapes

The swirling abrasive water jet nozzle is composed of a nozzle shell, twisted tape, mixing section, contraction section, and spreading section. The basic working principle of an ASWJ nozzle is: the fluid enters the mixing chamber through the twisted tape, which generates a swirl flow, pressurizes the nozzle contraction section, and forms a swirling jet with high central axial velocity and high peripheral tangential velocity under the restriction of the conical surface of the outlet spreading section.

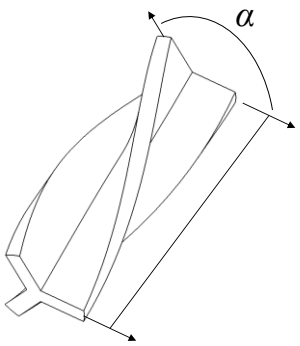

Fig. 2 Twisted tape and twisting angle

The twisting angle α is defined as the angle that the blade rotates along the axis. A series of tapes with 0°, 90°, 180°, 270°, 360°, 450°, 540°, 630°and 720° twisting angle were designed and geometric models was established.

3.2 Boundary conditions

In order to facilitate the analysis of application conditions of swirling abrasive jet nozzles, the steady-state numerical model established in this paper is based on the following basic assumptions:

1) Jet is un-submerged;

2) The phase parameters of pure water are consistent with those of water at standard conditions;

3) There is no impinging surface in the flow field.

Table 1 Boundary conditions and parameters values of the simulation

Parameters	Values
Inlet velocity/m·s^{-1}	5
Outlet pressure/MPa	0

At present, the experimental conditions are limited and non-submerged rock breaking experiments have been carried out. The assumptions set in this investigation is the non-submerged condition. This work can verify the flow field of rock breaking experiment under non-submerged condition.

According to the flow rate and the nozzle inlet inner diameter commonly used in the oil field, the velocity of the nozzle inlet was calculated and set at 5m/s. With sufficient mixing, the abrasive velocity distribution is often similar to the velocity distribution of the jet, so the abrasive phase is omitted. Based on the above consideration, numerical simulation boundary conditions of steady cases are set up (Table 1).

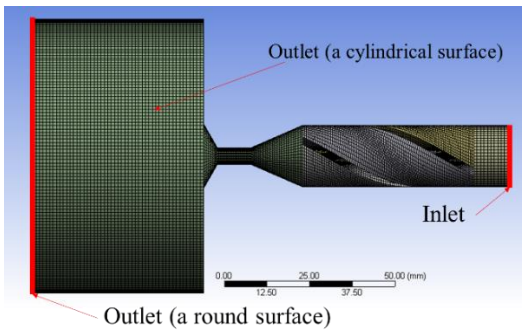

Fig. 3 Flow field and mesh of SAWJ nozzle

3.3 Grid independence

The flow field model of the SAWJ nozzle is composed of the inner nozzle field and the impingement flow field. Considering the actual working condition, the jet field outer the nozzle is designed as a cylinder. The whole mesh is of tetrahedral grids, which is suitable for fluid study.

Six groups of examples denoted G1-G6 of the different grid scales and the same case, and the number of G5-G6 grids is too large, resulting in a large cumulative error. G3-g4 has reached a stable calculated grid number, and 4×105 elements of G4 groups are the optimized group (Table 2).

Table 2 Grids independency test.

Groups	Number of Nodes	Dimensionless velocity of water	Deviation from the last mesh (%)	Pressure of water	Deviation from the last mesh (%)
G1	27241	47.15015	3.599	1109709	7.059
G2	53494	48.09328	1.671	1154544	3.303
G3	191358	48.53826	0.761	1175970	1.509
G4	429754	48.52617	0.786	1175276	1.567
G5	603337	48.6278	0.578	1180205	1.154
G6	1410654	48.91063	-	1193987	-

4. RESULTS AND DISCUSSIONS

4.1 Velocity

Section H/D =2 and Section H/D = 8 were selected to study the initial jet formation state and full development state of SAWJ flow. From the fig. 4, it can be concluded that water velocity magnitude profiles are of symmetry distribution, thus half of the profile area is selected to analyze the velocity. At H/D = 10 section the flow field study is introduced in section 4.2 by analyzing dynamic pressure. Where H the distance of the jet and D the diameter of the nozzle exit.

At H/D =2 section, the greater the twisting Angle α, the greater the radial velocity, indicating that the spreading performance is better. The axial, radial and tangential velocity profiles are all m-shaped. In the initial stage of jet formation, the maximum axial velocity distribution has little difference with a range of α=0°to α=270°. Along the jet axil, the axial velocity decrees with a range of α= 360° to α=720°. The greater the α is the radius where the maximum axial velocity occurs grows and the jet spreads more intense.

The radial velocity affects the spreading capacity of the jet directly, and the larger the radial velocity is, the more the fluid spreads in the radial direction. The radial velocity in the initial stage of the jet is directly proportional to the spreading capacity of the jet. At the full development stage, the radial velocity distribution has no obvious gradient and is at a low value. Jet spreading occurs mainly in the initial stage of the swirling jet flow. With the decay of tangential velocity, the fluid tends to move along the original direction in the full development stage of the jet flow.

At H/D =8, the radial velocity dissipates, and the spreading development slows down. After full development of the jet, while in the case with a larger twisted Angle, the lower the axial velocity is, and the higher the tangential velocity is. This is because the total momentum of the fluid is conserved and the increase of angular momentum will cause the decrease of axial momentum. The larger the jet distance is, the larger the axial and tangential velocity distribution diameter is. With a larger twisting angle α, the initial area of the jet to its full development, the tangential velocity decreased by more than half and the distribution radius doubled.

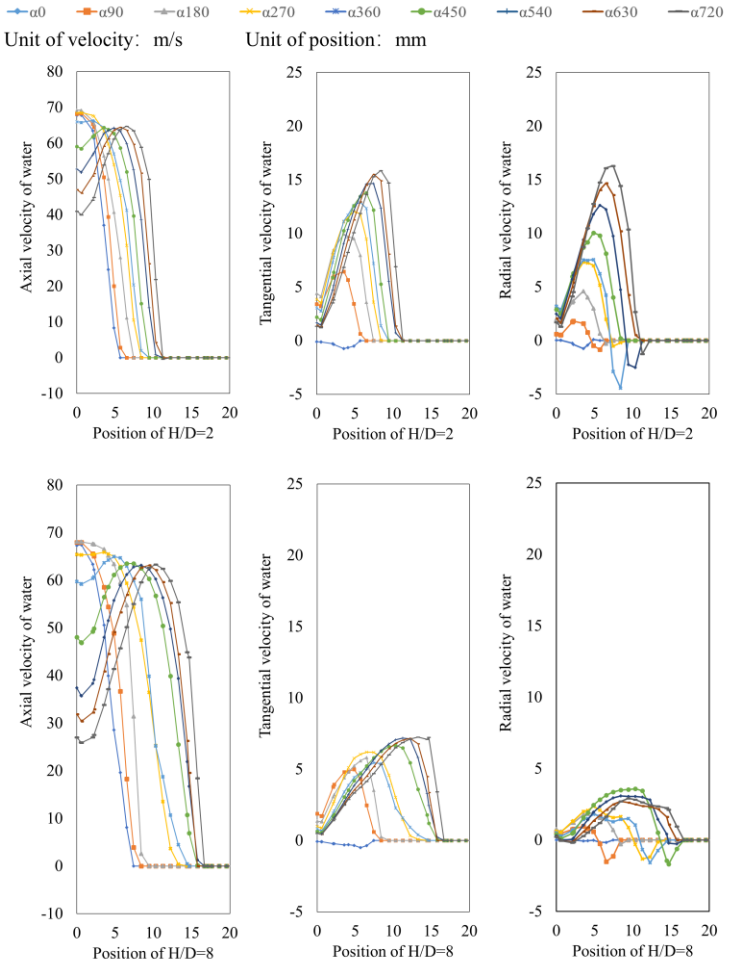

Fig. 4 Velocity distribution along the jet axis

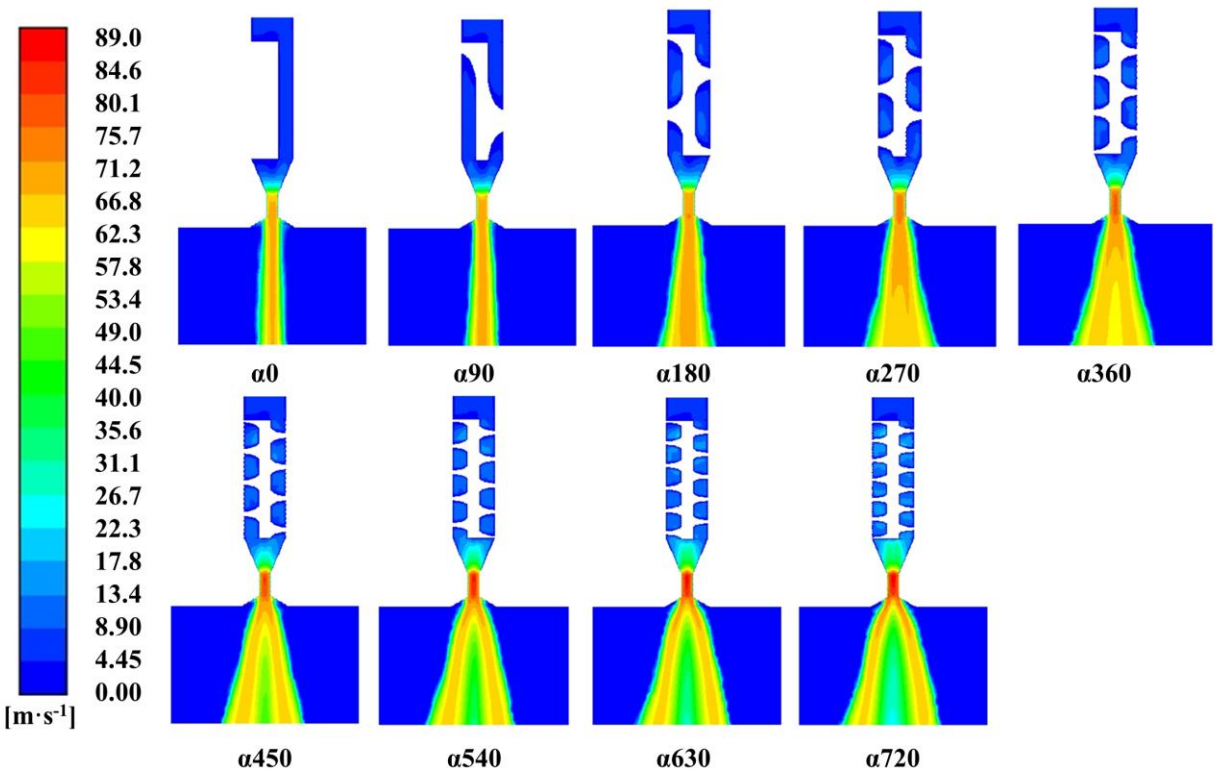

Fig. 5 Velocity magnitude profiles of the SAWJ flow field

Fig. 5 shows the velocity magnitude profiles of SAWJ flow field with a range of α=0°to α=270°. The velocity is getting higher at the contraction part because the axial velocity is accelerating to a high level due to the D and velocity magnitude is a combination of three-dimensional velocity components. With α higher than 180°, the potential core disappears in the jet flow field. With α higher than 360°, an obvious low-velocity area appears in the jet flow field. The spreading angle of SAWJ increases significantly which causes a lower velocity area.

4.2 Swirl number

Reynolds (Reynolds A.J. 1962) has shown that far away from the twisted tapes the width of the wake and consequently, the similarity scale depends on the ratio between the linear and angular momentum of the jet flow field. Formula (7) shows that the ratio between the linear and angular momentum can be denoted as a dimensionless parameter as swirl number S. Swirl number was calculated by a program written in codes, based on the formula (7) (Gong and Wang 2008). The U and W matrix was extracted out of the calculation solutions, then input into the swirl number calculation program.

As shown in fig. 6, among the jet axis, 0-10mm mixing chamber, 10-20mm contraction section, 25mm H/d=0 cross-section. Twisted tape generates a strong swirl strength, then decays along the jet axis. The swirling flow along the axis of blades with different twisting angles is studied. It is found that the greater the torsional Angle is, the greater the number of torsional spins will be. After fully mixing the axial shear velocity in the mixing chamber, the attenuation is quite drastic. In the contraction section, the S is steady and is a positive correlation to twisted angle α.

Fig. 6 and fig. 7 show that the spreading angle can be measured from the velocity magnitude profiles, three cases show that the twisting angle affects local swirl number at the nozzle exit. The spreading angle also is related to the local swirl number. The swirl number is directly related to the spreading capacity of jet flow, which further affects the well completion capacity of RJD.

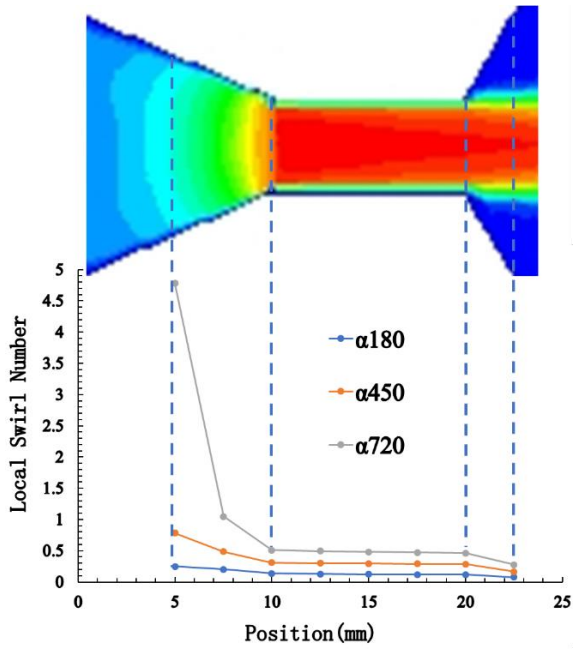

Fig. 6 Swirl number distribution along the jet axis

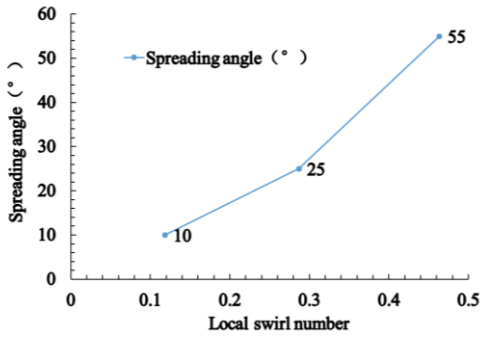

Fig. 7 Effect of Swirl number on spreading angle

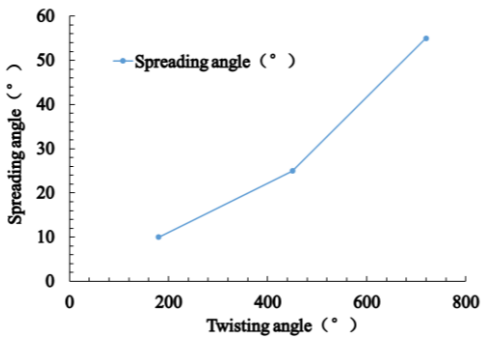

Fig. 8 Effect of twisting angle on spreading angle

4.3 Impinging pressure

In order to study rock breaking ability, dynamic pressure is extracted. The contour of dynamic pressure on the surface of H/d=10 distribution was plotted. The abrasive pressure distribution of α=0 is of round shape due to its poor mixing and poor spreading.

The dynamic pressure of the jet surface is distributed in an annular high-pressure region in the middle and a relative low-pressure region inside and around. The high velocity of the water phase results in high impact momentum. The dynamic pressure of 0-360° cases is of round distributed. With stronger α, the dynamic pressure of the water phase is of annulus distributed, and the pressure in the middle region is lower. This is because of the spreading effect at the full development stage on the surface.

The swirling flow can effectively expand the area of jet dynamic pressure by increase the radial momentum flux after jet impinging. The abrasive particles tend to push sideways rather than bounce back after impinging to the surface. The abrasive phase has greater destructive ability than the water phase, which further brings better rock-breaking effects. Therefore, it can be speculated that the SAWJ rock breaking effect is of round shape at a small jet distance and an annular at a large jet distance, forming a complete RJD wellbore with nozzle feeding in. In the rock breaking process, the central region will be destroyed by the impact force of the SAWJ. Under the action of abrasive erosion, damage around the central region will be larger than the jet diameter.

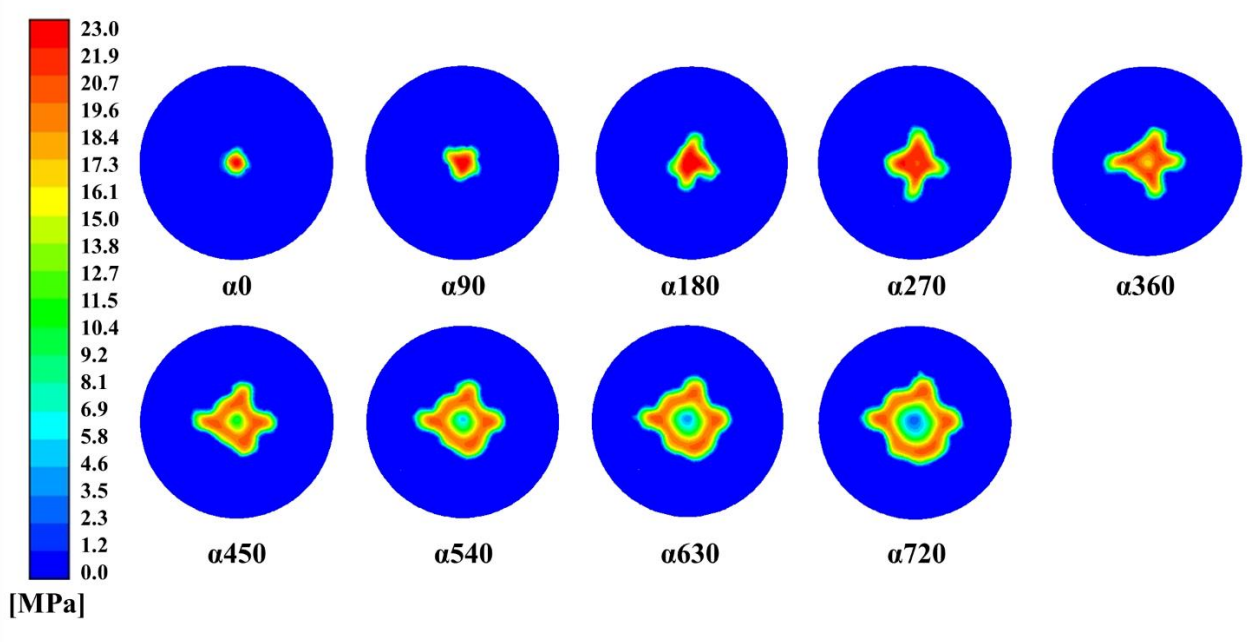

Fig. 9 Dynamic pressure of water jet

As shown in fig. 10 a SAWJ rock breaking experiment with 40-mesh quartz sand abrasive jet, 10MPa pump pressure, 3mm nozzle exit diameter, 360° twisted tape, H/D=10, 2 minutes jetting time. The experiment confirmed that the swirl flow adding with abrasive particles is able to form annular damage.

Table 3 Inner and outer diameter of dynamic pressure distribution

Twisting angle（°）	0	90	180	270	360	450	540	630	720
Inner diameter(mm)	-	-	-	2.8	5.4	9	12.7	14.9	18.3
Outer diameter(mm)	11.3	13.6	14.6	17.7	19.5	22.4	26.3	29	32.2

Fig. 10 SAWJ rock breaking effect

5. CONCLUSIONS

The jet flow of the SAWJ nozzle containing twisted tapes has been studied. The numerical results revealed that the twisted angle affects velocity distribution on the jet area. Before exiting the nozzle, the swirling number S changed greatly with twisted angle α, but after exit the nozzle, the S decays to a low value, and its spread degree was consistent with the S. A rock breaking experiment confirmed that the swirl flow is of annular-shaped.

6. ACKNOWLEDGMENTS

The research work was supported by the National Key Scientific Research Instrument Research Project of NSFC (No. 51827804) and Science Foundation of China University of Petroleum, Beijing (No. 2462018YJRC012).

REFERENCES

Ahmed, H. Kamel (2017): A technical review of radial jet drilling. In J. Petroleum Gas Eng. 8 (8), pp. 79–89. DOI: 10.5897/JPGE2017.0275.

Al-Marahleh G (2015): Parameters Controlling Abrasive Water Jet Technology: Erosion And Impact Velocity For Both Ductile And Brittle Materials.

Bang, Boo-Hyoung; Kim, Yong-Il; Ahn, Chan-Sol; Jeong, Seokgyu; Yoon, Youngbin; An, Seongpil et al. (2020): Theoretical model of swirling thick film flow inside converging nozzles of various geometries. In Fuel 280, p. 118215. DOI: 10.1016/j.fuel.2020.118215.

Debnath, Sudipta; Khan, Md. Habib Ullah; Ahmed, Zahir U. (2020): Turbulent swirling impinging jet arrays: A numerical study on fluid flow and heat transfer. In Thermal Science and Engineering Progress 19, p. 100580. DOI: 10.1016/j.tsep.2020.100580.

Gong, Chun; Wang, Zhenglin (2008): Commonly MATLAB language algorithm set. The first edition. Beijing: Publishing House of Electronics Industry (MATLAB Boutique series).

Gupta, A. K.; Lilley, D. G.; Syred, N. (1984): Swirl flows. Tunbridge Wells: Abacus Press (Energy and engineering science series).

Li, Jingbin; Li, Gensheng; Huang, Zhongwei; Song, Xianzhi; Yang, Ruiyue; Peng, Kewen (2015): The self-propelled force model of a multi-orifice nozzle for radial jet drilling. In Journal of Natural Gas Science and Engineering 24, pp. 441–448. DOI: 10.1016/j.jngse.2015.04.009.

Liao, Hua-Lin; Jia, Xia; Niu, Ji-Lei; Shi, Yu-Cai; Gu, Hong-Chen; Xu, Jun-Fu (2020): Flow structure and rock-breaking feature of the self-rotating nozzle for radial jet drilling. In Pet. Sci. 17 (1), pp. 211–221. DOI: 10.1007/s12182-019-00378-0.

Liu, Yanbao; Ba, Quanbin; He, Lipeng; Shen, Kai; Xiong, Wei (2020): Study on the rock‐breaking effect of water jets generated by self‐rotatory multinozzle drilling bit. In Energy Sci Eng 8 (7), pp. 2457–2470. DOI: 10.1002/ese3.679.

Patel K and Shaikh A. (Ed.) (2015): The Influence of Abrasive Water Jet Machining Parameters on Various Response – A Review.

Reynolds, A. J. (1962). Similarity in swirling wakes and jets. Journal of Fluid Mechanics Digital Archive, 14(02), 241-243.

Rohith NAIR; Lies E.PETERS; Saulius SLIAUPA; Robertas VALICKAS; Sigitas PETRAUSKAS (Eds.) (2017): A Case Study of Radial Jetting Technology for Enhancing Geothermal Energy Systems at Klaipeda Geothermal Demonstration Plant. 42nd Workshop on Geothermal Reservoir Engineering. Stanford University, Stanford, California, February 13-15.

S.-E. Kim; D. Choudhury; B. Patel. (Eds.) (1997): Computations of Complex Turbulent Flows Using the Commercial Code ANSYS Fluent. ICASE/LaRC/AFOSR Symposium on Modeling. Hampton,Virginia.

Salimzadeh, S.; Grandahl, M.; Medetbekova, M.; Nick, H. M. (2019): A novel radial jet drilling stimulation technique for enhancing heat recovery from fractured geothermal reservoirs. In Renewable Energy 139, pp. 395–409. DOI: 10.1016/j.renene.2019.02.073.

Shih, Tsan-Hsing; Liou, William W.; Shabbir, Aamir; Yang, Zhigang; Zhu, Jiang (1995): A new k-ϵ eddy viscosity model for high reynolds number turbulent flows. In Computers & Fluids 24 (3), pp. 227–238. DOI: 10.1016/0045-7930(94)00032-T.

Song, Xianzhi; Shi, Yu; Li, Gensheng; Yang, Ruiyue; Wang, Gaosheng; Zheng, Rui et al. (2018): Numerical simulation of heat extraction performance in enhanced geothermal system with multilateral wells. In Applied Energy 218, pp. 325–337. DOI: 10.1016/j.apenergy.2018.02.172.

Xu, Liang; Lan, Jin; Ma, Yonghao; Gao, Jianmin; Li, Yunlong (2017): Numerical study on heat transfer by swirling impinging jets issuing from a screw-thread nozzle. In International Journal of Heat and Mass Transfer 115, pp. 232–237. DOI: 10.1016/j.ijheatmasstransfer.2017.07.053.

Yang Yongyin; Shen Zhonghou; Wang Ruihe; Zhou Weidong (1999): Experimental Study On Rotary Abrasive Jet Drilling. In Petroleum Drilling Techniques (04), pp. 3–5.

Yang Yongyin; Shen Zhonghou; Wang Ruihe; Zhou Weidong (2005): Velocity profile of abrasive suspension swirling jet and influence of additive polyacrylamide (01), 34-36+40.